JACS
JOURNAL OF THE AMERICAN CHEMICAL SOCIETY

Perspective

pubs.acs.org/JACS

Pathogen Inhibition by Multivalent Ligand Architectures

Sumati Bhatia, Luis Cuellar Camacho, and Rainer Haag*

Institut für Chemie und Biochemie, Freie Universität Berlin, Takustrasse 3, 14195 Berlin, Germany

ABSTRACT: Interfacial multivalent interactions at pathogen−cell interfaces can be competitively inhibited by multivalent scaffolds that prevent pathogen adhesion to the cells during the initial stages of infection. The lack of understanding of complex biological systems makes the design of an efficient multivalent inhibitor a toilsome task. Therefore, we have highlighted the main issues and concerns associated with blocking pathogen at interfaces, which are dependent on the nature and properties of both multivalent inhibitors and pathogens, such as viruses and bacteria. The challenges associated with different cores or carrier scaffolds of multivalent inhibitors are concisely discussed with selected examples.

INTRODUCTION

Multivalency is a ubiquitous phenomenon in nature that involves complex binding mechanisms for achieving noncovalent strong yet reversible interactions between *m*-valent ligands and *n*-valent receptors (where $m, n > 1$). Multivalency can be seen in the form of a burr or man-made Velcro brand fasteners as a common principle in nature, where multiple flexible hooks interact with a filamentous surface. Multivalent interactions play a decisive role in biological systems for the self-organization of matter, recognition, adhesion, and signaling processes.[1−3] Understanding multivalent interactions on the molecular level is of prime importance for developing optimized multivalent ligands to achieve a strong biological effect. Individual carbohydrate−protein interactions have typically low affinity, with a dissociation constant (K_d) ranging from μM to mM concentrations. Such weakly binding carbohydrate ligands are present in a multivalent format on the cell surface, for example, in the form of glycolipids, which enhance the attractive binding forces and at the same time permit several dissociative events to perform a variety of biological functions. The receptor−ligand binding or the receptor cross-linking affects the intensity and duration of signaling events.[4,5] Multivalent ligands can cross-link membrane receptors much more efficiently and regulate the signaling process.[6,7] Another example of multivalent interactions from nature is the adhesion of pathogens like virus,[8,9] bacteria,[10,11] or fungi[12,13] to host cells, which is the very first step in the infection process. Viruses, for example, adhere to cell surface receptors by multivalent interactions and are subsequently taken up by the cells, often by endocytosis, to deliver genetic material and make new copies of infectious particles.[8,9] Protein−carbohydrate interactions play an important role for pathogen adhesion to cells. Various unnatural glycoconjugates (neoglycoconjugates) have been synthesized with different spatial arrangement of ligands in an attempt to prevent infection.[14] Examples of ligands include sialic acid for influenza,[15] high-mannose-type glycans to interfere with HIV and DC-SIGN interactions,[16] α-D-galactose and L-fucose for cytototoxic lectin A and B, respectively, produced from *Pseudomonas aeruginosa*,[17,18] α-mannoside and galabiose for FimH[19] and p-fimbriae,[20] respectively, expressed on *Escherichia coli*, monosialotetrahexosyl ganglioside (GM1 oligosaccharides) for cholera toxin (CT),[21] P^k saccharide for shiga-like toxins (SLTs),[22] and many more.

Current therapies require high doses of small drug molecules. Monovalent drugs—for example, Tamiflu or Relenza against influenza and various antibiotics against different bacterial or fungal infections—are being constantly used to treat such infections and can lead to drug resistance in patients.[23,24] Optimized multivalent inhibitors, which not only bind to several receptors on pathogens but also shield them, can be used to completely inhibit the pathogen adhesion to the cell surface (see Figure 1).[25−30] Multivalent inhibitors do not kill pathogens but can block them from binding to cells, which can reduce the chances of developing drug-resistant strains. Pathogens bound to multivalent ligands can no longer replicate and can be degraded by macrophages or cleaned off by the reticulo-endothelial system,[31−33] but there has not been any study reported so far on the fate of multivalent ligand−pathogen complexes in biological systems. The efficiency of this competitive inhibition greatly depends on the enthalpic and entropic contributions, but precise theoretical modeling of thermodynamic and kinetic parameters is usually hampered by the complexities of the biological systems.[34,35] However, the concept of multivalent inhibitors as drugs (or prophylactics) has not been recognized by the pharmaceutical industry because the optimization of reproducible polymeric multivalent ligand is practically more challenging than that of the standard monovalent drugs. Another important question to be addressed is whether the multivalent ligand pathogen binder can be applied in the late stages of infection when a pathogen has already started replicating in the biological system. In a study by Matrosovich et al.,[36] multiple treatments with aerosolized polyacrylamide-based glycopolymer on days 2−5 post infection increased the survival of influenza-virus-infected mice. This study showed the applicability of this polyvalent inhibitor of virus attachment for both prevention and treatment of influenza. Despite past efforts to develop multivalent glycoconjugates as drugs, only a few examples from *in vivo* studies have been reported.[37,38] Toxicity, biocompatibility, and low *in vivo* efficacy are important concerns for the applicability of multivalent glycoconjugates for clinical studies. However, there are a few successful examples of multivalent glycoconjugates as

Received: December 11, 2015
Published: June 24, 2016

DOI: 10.1021/jacs.5b12950
J. Am. Chem. Soc. 2016, 138, 8654−8666

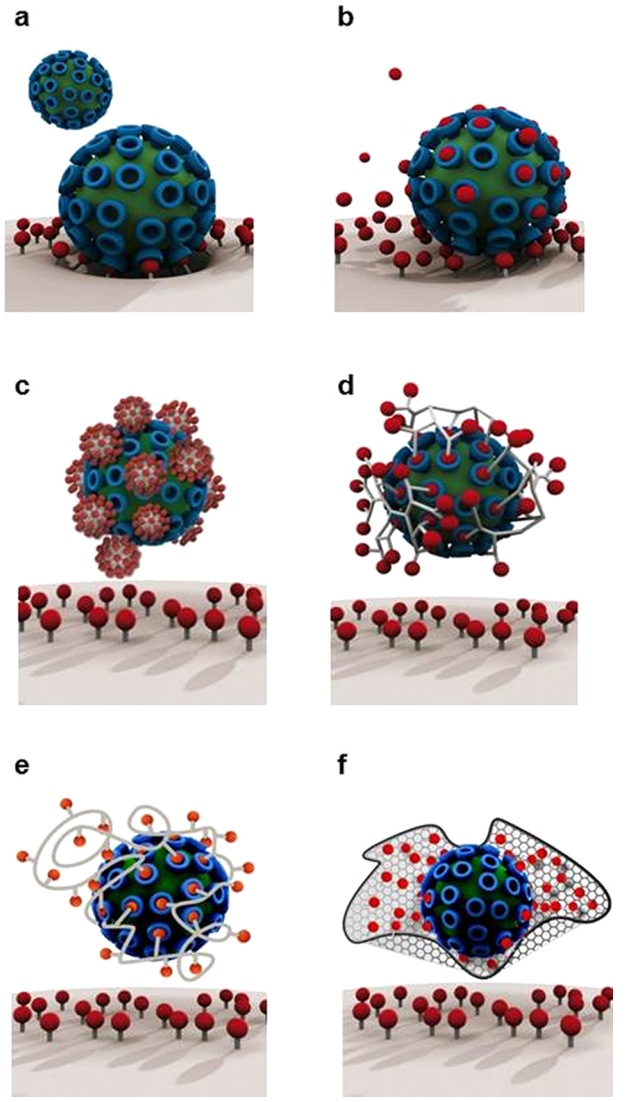

Figure 1. (a) Multivalent binding of a virus to the cell surface is compared to (b) monovalent inhibition using a classical drug approach where the virus binds to the cell despite the presence of high doses of monovalent drugs (red). (c) A globular multivalent inhibitor decorated with ligands (red) binds to the virus surface and accesses a limited number of receptors due to its rigidity. (d) Dendritic and star-like polymers can be highly adaptive and considerably more effective in binding and shielding a virus surface than monovalent ligands, thus preventing viral adhesion. (e) A random coiled linear polymer with molecular weight similar to that of a globular inhibitor decorated with ligands (red) can stretch and attain different conformations to access a higher number of receptors, and thus sterically shield some of the receptors from undesired interactions. (f) A flexible multivalent 2D scaffold decorated with ligands can strongly interact with the virus and shield the virus efficiently. Parts (a), (b), and (d) are adapted with permission from ref 1. Copyright 2012 Wiley-VCH Verlag GmbH & Co. KgaA.

drugs or vaccines. For example, a synthetic glycolipid analogue, Synsorb-Pk, that was covalently attached to a silica particle has emerged as an anti-adhesive drug candidate for absorbing SLTs of *E. coli*.[39,40] The phase II clinical trials with this candidate showed 54% reduction in the risk of developing hemolytic uremic syndrome if this drug is started within 3 days of the onset of diarrhea.[41] Other advances in generating the recombinant *E. coli* that displays on its surface a lipopolysaccharide (LPS) that mimics the shiga toxin receptor showed improved binding and efficacy over Synsorb-Pk.[42−44] Another example is an octavalent *O*-polysaccharide (OPS) with toxin A conjugate that was found to be immunogenic and effective against *P. aeruginosa* and is currently undergoing phase III clinical trials as a vaccine candidate.[45] In this Perspective, we have focused on the understanding of multivalent interactions from the molecular level to bigger platforms and have highlighted the challenges and concerns in targeting multivalent interactions. Multivalency has the potential to bring forward powerful anti-infective drugs as well as other strong binders.

MULTIVALENT LIGAND/PLATFORM DESIGN

The ligand and platform design are of central importance in the field of multivalency to inhibit undesired interactions by specific attachment to a target protein, macromolecular assembly, pathogen, or cell. For this reason, considerable efforts have been made to appropriately design molecular inhibitors that can accurately fit into a particular biological situation to achieve not only high affinities but also a quantifiable inhibition.[46]

During the monovalent interaction, a ligand diffuses in solution to find and bind a receptor with a free energy of interaction $\Delta G = \Delta H - T\Delta S$, where ΔG is the free energy of binding and is the sum of enthalpic (ΔH) and entropic ($-T\Delta S$) contributions. While enthalpic changes account for the strength of the interaction independently of its origin (hydrogen bonding, van der Waals forces, electrostatic, etc.), the entropic term $-T\Delta S$ includes the changes in degrees of freedom lost or gained during the formation of the complex. The release of water molecules from the binding site caused by hydrophobic interactions imposes an additional entropic contribution to the free energy during binding. The change in entropy, therefore, can be written as $\Delta S_T = \Delta S_{tran} + \Delta S_{rot} + \Delta S_{conf} + \Delta S_{solv}$. The first three terms refer to the changes in translational, rotational, and conformational degrees of freedom of the ligand before and after formation of the complex. ΔS_{solv} represents the change of entropy due to the removal of organized water molecules within the binding pocket during the binding process.[47,48]

To obtain a deeper comprehension of the thermodynamic features governing multivalency, researchers naturally extended monovalent cases to multivalent ones in recent years. The main difference between a monovalent ligand and its multivalent counterpart is that the binding is mostly an enthalpy-driven process in the former case, whereas, in a multivalent interaction, the scaffold itself and the spacer linking the multiple binding groups incorporate significant entropic penalties arising from their own intrinsic degree of conformational flexibility. For instance, scaffolds can be hard or soft and spacers can be rigid or flexible. An enhancement factor β, which was proposed by Whitesides and co-workers to characterize the multivalent binding effect without knowing the exact number of interaction sites, is the ratio of the binding constant for the multivalent binding [K_{multi}] of a multivalent ligand to a multivalent receptor and the binding constant for the monovalent binding [K_{mono}] of a monovalent ligand to a multivalent receptor.[49] This enhancement factor is quite useful for obtaining an idea of the impact of multivalent binding in biological situations, since it also includes the influence of cooperativity and the symmetry effect. A multivalent binding site can be non-cooperative (additive), positively cooperative (synergistic), or negatively cooperative (interfering). Cooperativity effects for different multivalent systems have been corrected by Stoddart,[50]

DOI: 10.1021/jacs.5b12950
J. Am. Chem. Soc. 2016, 138, 8654−8666

Reinhoudt,[51,52] Schneider,[53] and Brewer.[54] Thermodynamic analysis of the "multivalency effect" for the binding of different multivalent carbohydrates to lectins showed associated negative cooperativity.[54] Studies by Stoddart and co-workers[50] on different supramolecular systems for host−guest interactions proved multivalent interactions to be negatively cooperative. The positive cooperativity is typically associated with allosteric systems where the binding of the first ligand leads to a conformational change in the host to accommodate the second ligand with higher affinity than the first one. The best example for such behavior is the allosteric binding of four oxygen molecules with tetravalent hemoglobin.[55] Multivalency, therefore, should not be confused with the cooperativity. Multivalent interactions are mostly negatively cooperative but still much more efficacious than those of the corresponding monovalent ligands.

In the past two decades, various techniques have been used to quantitatively understand multivalent interactions from a molecular level to the full adhesion of two multivalent surfaces. On the one hand, isothermal titration calorimety (ITC),[56−59] surface plasmon resonance (SPR),[60−62] quartz crystal microbalance (QCM),[63−65] and microscale thermophoresis (MST)[66−68] techniques were used to obtain affinity constants in ligand−receptor complexes where an individual or multiple binding occur. Even though valuable thermodynamic data can be extracted with these methods, the main drawback of these approaches is that the multivalent features from heterogeneous binding species cannot be always fully discriminated, and characteristic features of monovalent binding remain often obscured. On the other hand, highly sensitive techniques using, for example, a surface force apparatus (SFA),[69,70] biomembrane force probe (BFP),[71,72] atomic force microscope (AFM),[73,74] and optical tweezers (OT)[75,76] were applied to measure the minute forces required to break the individual non-covalent bonds. These force spectroscopic data have provided unique insight into the mechanistic aspects of the induced single-molecule bond dissociation. Applying theoretical models borrowed from reaction kinetics on these data makes it possible to extract main bond characteristic parameters like kinetics off-rates k_{off}, bond trap depth x_{β}, and bond lifetime τ.[77,78] An obvious advantage of these single-molecule methods is the direct identification of the binding members in multivalent interactions. In most cases, however, learning from individual bond ruptures in specific ligand−receptor interactions does not render an accurate determination of the binding affinities (K_d) between interfaces bearing the same monovalent binding partners. Simple additivity of pair-binding interactions will not necessarily explain the whole binding affinity. An accurate determination of the dissociation constant (K_d) between both interacting interfaces is not straightforward, and applying reliable approximations is possible only under certain circumstances.[79,80]

The first binding event between multivalent ligands and receptors produces spatial proximity and significantly determines the probability of the subsequent binding process. The binding process can be evaluated kinetically in terms of association rate k_{on}, which is a diffusion-limited parameter and a weighted average quantity for many elementary binding processes during multivalent interactions.[1] The kinetic studies, with several examples in the literature, have demonstrated that multivalent interactions do not always significantly affect k_{on}, but the dissociation occurs more slowly in multivalent systems than in the analogous monovalent ones. So the significantly lower dissociation rate k_{off} determines the large differences in K_d values of the multivalent and the corresponding monovalent system. For example, a recent binding kinetic study by Tan et al. has shown that the relative k_{off} value of bivalent 15-base aptamer (15-Apt) for thrombin binding is 51.7 times lower than that of monovalent 15-Apt, whereas bivalent 15-Apt exhibits only 1.2 times higher relative k_{on} than the monovalent 15-Apt. The K_a of bivalent 15-Apt was ∼62 times stronger than that of the free 15-Apt.[81] Other studies, with multivalent nanoparticles with weakly binding monovalent groups, by Li and Tassa have demonstrated that the k_{on} values do not considerably change even when there is a pronounced variation and increase in the calculated K_d.[82,83] Multivalent nanoparticles seem to increase the multivalent capacity at the site triggered by the contact time the interfaces face each other, but only after the binding of the first single (or a few) monovalent interactions. However, the interaction of a multivalent inhibitor with its target can have a more complex thermodynamic and kinetic behavior. A recent study by Munoz et al. on binding kinetics showed that the contribution of binding mechanisms is dynamic in nature and varies with the local concentration of glycoconjugates nearby the lectin surface.[84] Their results show the importance and the need of understanding kinetics at the interface in multivalent interactions, which remains still largely unexplored and plays a pivotal role in improving the design of multivalent inhibitors.

The spacer and scaffold are common components of a multivalent inhibitor, which have to be optimized to reduce the thermodynamic penalties imposed by undesired conformational degrees of freedom that could impede binding. The spacer length and scaffold size should be designed to match and connect the opposite ligand−receptor pairs with increased "on" rate due to faster binding against a compatible surface, and decreased "off" rate through continuous rebinding of the binding groups fixed at the close proximity. Such an optimized multivalent inhibitor will consequently possess a longer lifetime during binding to its target as a whole as compared to the individual monovalent ligands.

An intelligent design of a multivalent inhibitor requires knowledge of the intrinsic affinity of ligands for the receptor, and also of the size, shape, and receptor distribution on the target surface. Inhibition of pathogen adhesion to cells not only arises because of high affinities of multivalent ligand−receptor interactions but also is due to other effects like steric shielding, clustering, statistical rebinding, etc.[85] Different carrier backbones can be selected, ranging from small scaffold-like dendrimers, nanoparticles, nanogels, or bigger microgels (3D) to micrometer-sized bigger platforms (2D), depending on the size and properties of the targeted pathogen. Enhanced binding affinities, steric shielding effects, and various other mechanisms play an important role for the prevention of pathogen adhesion. Figure 1 describes a general situation where a big spherical pathogen, for example, a virus, is targeted by different multivalent architectures, such as a globular hard sphere or dendritic polymer, linear (random coil) polymer, and a flexible 2D scaffold with a size similar to or bigger than that of the pathogen itself. Considering the same molecular weight linear and hyperbranched multivalent scaffolds under optimized conditions, one may expect that the linear flexible scaffold can access a higher number of receptors than a relatively rigid globular or hyperbranched scaffold. Linear scaffolds can attain different conformations, thus not only making more ligand−receptor bond pairs but also sterically shielding some areas of

DOI: 10.1021/jacs.5b12950
J. Am. Chem. Soc. 2016, 138, 8654−8666

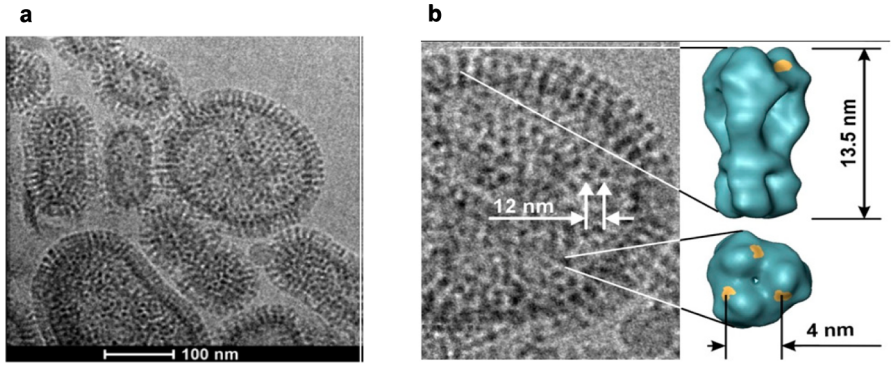

Figure 2. (a) Cryo-TEM image of influenza A virus ($X31/H_3N_2$) showing the abundant distribution of hemagglutinin (HA) glycoprotein trimers on the virus surface. (b) Inter-trimeric distances and length of the stem domain of HA_3 indicated as observed in the TEM image. Yellow patches on the globular domain of HA trimers show the receptors for the sialic acid sugar residues. Part (b) is adapted with permission from ref 143. Copyright 2010 Wiley-VCH Verlag GmbH & Co. KGaA.

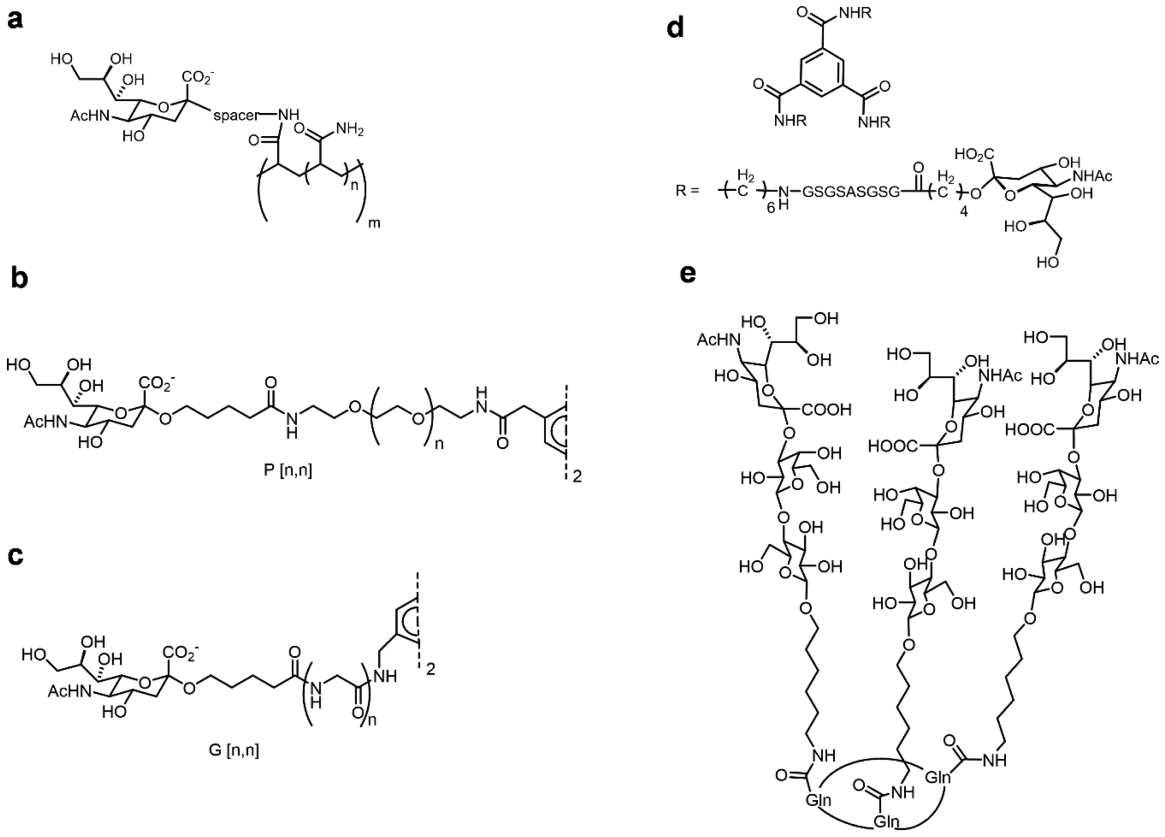

Figure 3. (a) Multivalent sialoside on polyacrylamide backbone. (b) Bivalent sialoside with polyethylene glycol spacers of different lengths (P series). (c) Bivalent sialoside with oligoglycine spacers of different lengths (G series). (d) Trivalent sialoside with alkylated peptide backbone. (e) Trivalent sialyllactose on cyclic peptide template.

the pathogen. The bigger, adaptable, ligand-decorated 2D scaffold may have great use in wrapping up bigger pathogen-like micrometer-sized bacteria, although there are several issues to be addressed while using them as inhibitors in biological systems (see Figure 1). The size, shape, and also inhibitor-to-pathogen size ratio play crucial roles in determining the binding mechanism.[85,86] A variety of multivalent ligand architectures have been explored in the past, but only a few systematic comparative studies using different scaffold architectures have been reported for understanding the influence of backbone architectures on multivalent interactions. Here, we discuss optimization of different parameters for targeting pathogens, with some selected examples from the literature.

LIGAND DENSITY

The overall affinity of the multivalent inhibitor can be modulated by varying the ratio of active ligands to inactive functional groups on their carrier backbone. Ligand density is an important parameter to be optimized, because too low or too high ligand density can drastically affect the inhibitory potential of the scaffold. Knowledge of the topological receptor distribution profile on the target/pathogen surface can be helpful for designing a multivalent inhibitor with a particular

DOI: 10.1021/jacs.5b12950
J. Am. Chem. Soc. 2016, 138, 8654−8666

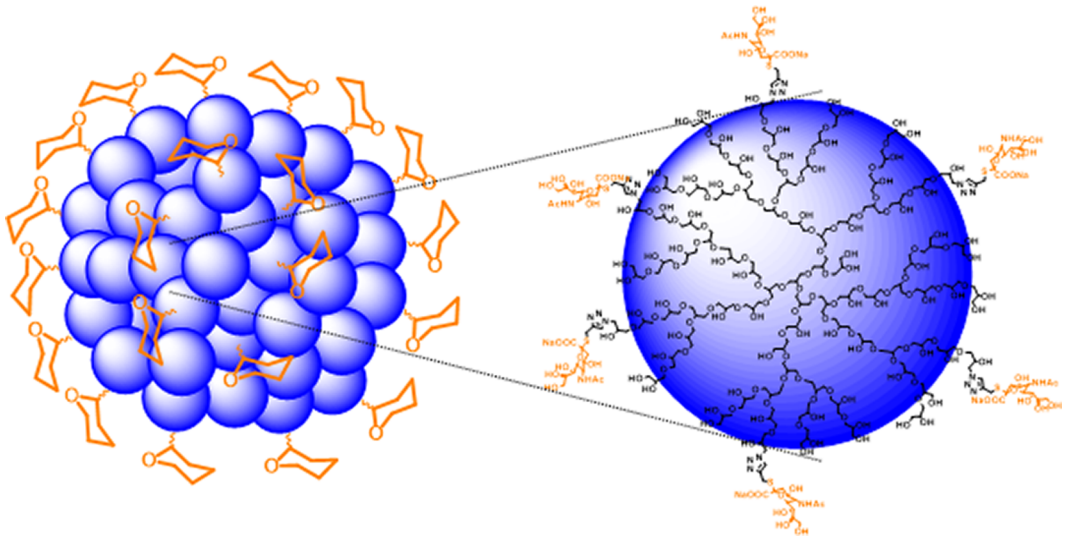

Figure 4. Sialic-acid-functionalized polyglycerol nanogels (nPG) with hemagglutinin receptors on the virus surface. The nPG consists of a number of chemically cross-linked dendritic polyglycerol (dPG) units. Reprinted with permission from ref 2. Copyright 2014 The Royal Society of Chemistry.

chemical construct and ligand density, for instance, if the receptors are uniformly distributed and exposed or present in clusters on the pathogen's surface. The influenza virus, for example, has a nearly uniform distribution of hemagglutinin (HA) glycoproteins on the virus surface. A typical influenza virus with a diameter of 120 nm has around 400−500 copies of HA trimeric proteins, each with three binding sites for SA on its globular domain. The planar distance between the binding sites on a single HA_3 is around 4−5 nm, whereas the distance between the centers of the adjacent heads of HA_3 trimers is 10−12 nm (see Figure 2).[87−91]

Several multivalent sialylglycopolymers have been investigated in detail to inhibit the influenza virus. Initially, α-sialoside-polyacrylamide copolymers were extensively studied by Roy and Whitesides to inhibit the agglutination of erythrocytes by influenza A virus (see Figure 3a).[92−94] In one of the reported studies, the best copolymer in the series inhibited hemagglutination 10^4−10^5 times more strongly than did similar concentrations of α-methyl sialoside. The virus inhibition was found to depend on the content of sialic acid on the polymeric backbone. Polymers containing *O*-glycosides at intermediate values of mole fraction of sialic acid residues (χ_{SA} = 0.2−0.6) were more potent inhibitors of hemagglutination than those with higher or lower degrees of functionality.[94] In one study, our group found that 50-nm-sized sialic-acid-conjugated nanogels with only 12% ligand density were the best and showed 80% inhibition of the influenza A virus (strain A/X31), while high ligand density led to loss in binding efficiency (see Figure 4). An optimum spacing between the ligands, therefore, is essential for maximum efficiency in binding per ligand.[25] Controlling the ligand density per nm^2 is also a good approach for obtaining optimum density for nanoparticle inhibitors. Expression of inhibitory potency of the multivalent compound in terms of ligand concentration, therefore, will be essential to assess the impact of multivalent ligand presentation on the architecture.

Although multivalent inhibitors with statistical distribution of ligands on the polymeric backbone were proven to be effective pathogen inhibitors, several efforts have been taken for an accurate ligand design to match the dimensions of the protein-binding pocket using the precise knowledge of protein ultrastructure. Accurate ligand design provides a better understanding of the influence of different factors, like length and flexibility of spacer, valency, and spatial orientation of ligands, on multivalent interactions. Knowles and Glick investigated two series of bivalent sialosides with polyethylene [P(*n*,*n*) series] and oligoglycine [G(*n*,*n*) series] as spacers with different lengths (see Figure 3b,c).[95] The bivalent inhibitor with glycine spacer (n = 4) bound 5-fold better than the compound with polyethylene glycol (PEG) spacer (n = 4) and 100-fold tighter than the monovalent sialic acid when tested for hemagglutination inhibition using the whole virus. No decrease in K_d was observed when the same compounds were tested using bromelain-released HA. This study showed the intermolecular binding of bis-sialosides to adjacent HA trimers.

An early example of the trivalent system was provided by Whitesides and co-workers, where tris(vancomycin carboxamide) (V_3) showed exceptionally high affinity ($K_d = 4 \times 10^{-17}$ M) for the ligand derived from D-Ala-D-Ala (DADA) (L).[96] ITC studies indicated the enthalpy association of −40 kcal/mol, about 3 times that of V+L, and thus entropy of association −18 kcal/mol, about 4.5 times that of V+L. In an ideal case for a trivalent system to afford high binding constants, conformationally stiff spacers should be accurately designed for ligand−receptor interactions with minimal loss in conformational and rotational entropy on binding, and also the inclusion of a hydrophobic component can give a large positive contribution from $T\Delta S$ from release of water.[96]

A recent example of these precisely crafted multivalent inhibitors is the generation of alkylated peptide units displaying triads of SA that have been designed to fit within a single HA head of the influenza virus (see Figure 3d). Here, peptide linkers were chosen instead of commonly used ethylene glycol oligomers to reduce overall flexibility, which in turn reduces the entropic cost during binding. The optimized tripod had 4000-fold increased affinity (K_d = 450 nM) for H5 of avian influenza as compared to the Neu5Acα2Me, which is the interaction strength between bi- (500-fold) and trivalent (~300 000-fold) ligands.[97] Another study, by Ohta et al., showed that a 3D arrangement of the multidentate ligand, which was determined by the scaffold, was significantly important for achieving high affinity for the HA protein.[98] They observed that the tridentate

DOI: 10.1021/jacs.5b12950
J. Am. Chem. Soc. 2016, 138, 8654−8666

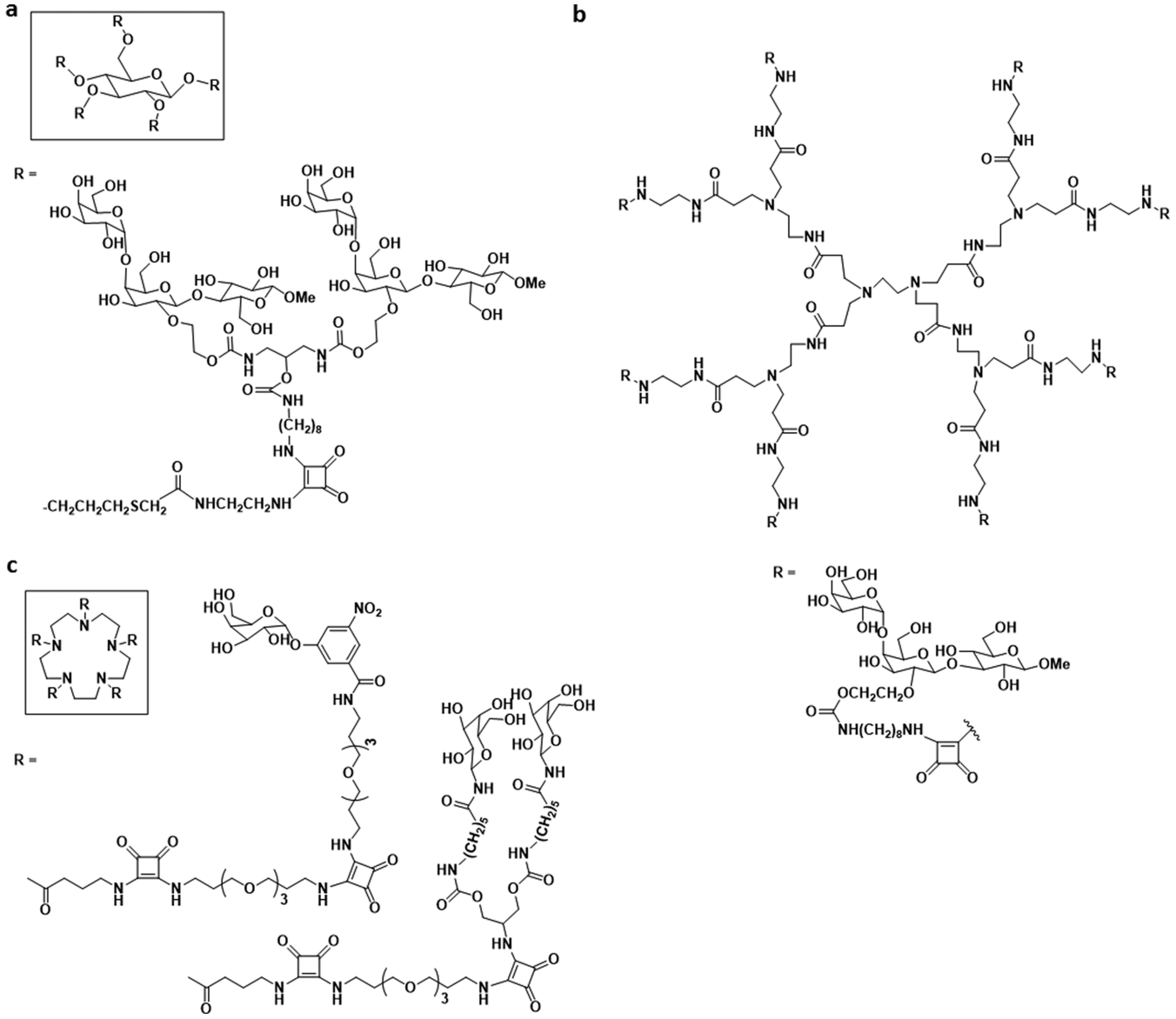

Figure 5. (a) Structure of a decavalent starfish inhibitor of Shiga-like toxins. (b) Structure of an octavalent inhibitor of Shiga-like toxins. (c) Multivalent (single and branched) galactose binders for cholera toxin.

sialyl lactose ligand on a particular cyclic peptide template, where all the three ligands were directed outward from the cyclic peptide ring, exhibited highest affinity (K_d = 0.65 mM) for HA protein on the SPR sensor surface (see Figure 3e).

Here, the distance between binding sites on the HA structures needed to be known in advance in order to simultaneously bridge and reinforce the bond formation between the tripod units and binding pockets at the HA head. Using longer PEG segments not only raised the probability of the ligand and receptor binding, but also greatly increased the entropic cost through molecular conformations of the tethered chains. Usually models like the worm-like chain or the freely jointed chain model that account for the mechanical properties of the spacers are used to describe their degree of flexibility and fluctuating dynamics while in solution.[99,100] Using flexible oligoethylene glycol (OEG) segments in a tripod would increase the adaptability of this inhibitor to fit its target, but at the expense of a large entropic cost due to an inevitable increase of molecular conformations of the tethered chains. Even when the length of these flexible spacers is designed to match the distances between binding sites, the final binding affinity could still be lower than that of a monovalent ligand, because the large fluctuations of the spacers could drastically reduce the binding probability. Bujotzek et al. carried out a computational analysis for the conformational entropy of spacers with different flexibility in bivalent inhibitors for the estrogen receptor.[101,102] It was concluded from their results that the probability of finding a bivalent ligand in an extended state is low due to the gain in conformational entropy. Similar arguments would apply for spacers in tripod structures.

A prominent example of an approach to design bivalent ligands with variable spacer length was reported by Abendrot.[103] In this study, a DNA segment was used as a spacer to precisely control the distance between the ligands matching the estrogen receptor. The selective estrogen receptor modulators 4-hydroxytamoxifene and raloxifene were used as ligands and were covalently bound to a DNA strand of length similar to that of the receptor binding pockets. Binding affinity

DOI: 10.1021/jacs.5b12950
J. Am. Chem. Soc. 2016, 138, 8654−8666

was found to be clearly affected by the spacer length. A remarkable increase in the relative binding affinity (RBA) of up to 300% was found. The bivalent ligand showed binding affinities 5−7 times higher than the monovalent association which proved the advantage of bivalent presentations with an optimized spacer.

Through the creation of excellent multivalent binders that match the topology of the receptor protein structure, e.g., starfish-like inhibitors, a deeper understanding of multivalency was gained.[104−109] These molecules with their planar and radially distributed binding sites have shown their potency to block the interaction of planar homopentameric subunits present in bacterial toxins like cholera and Shiga.[110,111] These studies were further expanded from a matched pentavalent inhibitor to octa- and decavalent systems for AB_5 toxin (see Figure 5). A thermodynamic model was provided by Bundle and Kitov to explain the enhancements in AB_5 toxin inhibition for the situations where several statistical options for binding are available.[112] A statistical term, "avidity entropy", was introduced to describe how many ways a multivalent ligand can bind to multiple binding sites. This explained the higher inhibitory potency of an octavalent system than the pentavlent one for SLT.

Turnbull and co-workers, furthermore, unraveled the influence of mismatched valency on aggregation mechanism for inhibiting bacterial toxins.[113] Structural studies employing atomic force microscopy (AFM) showed that the divalent GM1 analogue induced head-to-head dimerization of the protein toxin and caused protein aggregation, but the use of the tetravalent GM4 analogue did not display any protein aggregation. A recent study by Pieters and co-workers showed that an inhibitor with mismatched valency could be used that was just as potent as the 1:1 design approach for toxin inhibition. In this study, tetravalent and pentavalent CT inhibitors based on a closely related scaffold were found to be equally potent for CT inhibition.[114] The reason was attributed to the possibility of more geometries and their ability to form higher order structures due to more statistical options for binding.

A maximum binding affinity for these systems, therefore, requires an appropriate balance between the conformational entropy of the flexible chains and the enthalpic contribution due to simultaneous binding. Simulation studies using molecular dynamics or Monte Carlo have already shed light on mechanistic aspects during the above-mentioned bond formation, and will provide more information regarding final binding affinities in the years to come.[115−117]

MECHANICAL PROPERTIES OF PATHOGENS

The mechanical property of the target is an important issue that must be taken into account when anticipating the binding events in the different scaffold architectures. For example, the genome can be protected in viruses solely by a protein shell displaying the binding groups on its surface. In other cases, this protein shell or capsid is wrapped within a lipid membrane from which the surface proteins spike out on the surface. Representative examples of both these cases are rhinovirus for non-enveloped and influenza for enveloped viruses. Susceptibility to deformation of a virus particle or a capsid is still being researched, but experimental studies have shown that it strongly correlates to the virus life cycle.[118−122] Stiffness of the virus can drastically change when the virus is exposed to different environmental conditions, i.e., different pH, ionic strength, etc. An effective multivalent inhibitor must then maximize its binding capacity by possessing an array of ligands matching that of the virus surface and increasing its contact area upon binding. Strong multivalent attachment between inhibitor and pathogen will then be strengthened in the following cases: (a) when both interfaces possess a soft core that permits an increase in the contact area but the large entropic cost also has be considered for higher affinity, (b) if the ligand density of the inhibitor mimics that of the pathogen surface, and (c) if the intrinsic binding affinity per bond is high. These different scenarios are obviously intertwined, and depend on the mechanical properties of the inhibitor scaffold and the pathogen.

Single-virus binding studies by Rankl et al. have demonstrated the multivalent attachment of non-enveloped rhinovirus with low-density lipoprotein receptors (LDLR).[123] They found binding forces of about 82 pN for a single virus-receptor bond. Using a single-molecule method, Sieben et al. measured the unbinding forces between individual influenza virions and their receptors on the cell surface.[124,125] The force spectroscopic data obtained clearly showed that the influenza virus utilizes a multivalent attachment on the surface of the cell characterized as a zipper-like mechanism during unbinding. They found that forces of about 10−25 pN are required to break single bonds between HA and its sialic acid receptors present on the cell surface (see Figure 6). This force per bond is significantly lower

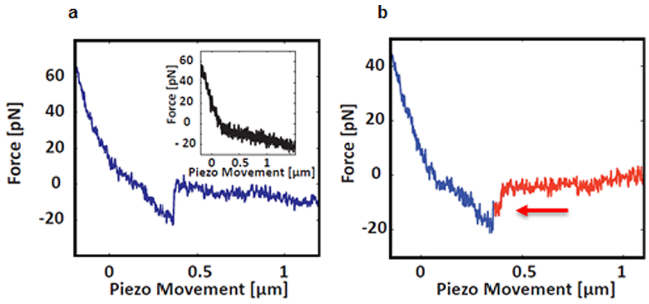

Figure 6. Single virus force spectroscopy (SVFS) measured by AFM in force spectroscopy mode. (a) The interaction between virus and a single receptor; no interaction could be observed when the cantilever was blocked with BSA (a, inset). (b) Interaction of virus with multiple receptors produced serial rupture events (b, arrow). Adapted with permission from ref 125. Copyright 2012 National Academy of Sciences.

than that in a single rhinovirus binding interaction. Due to its smaller size and reduced number of binding sites during contact, it is possible that rhinovirus compensates its lack of multivalency compared to the influenza virus by increasing the binding strength per bond. This could represent a general strategy utilized by pathogens with a fewer number of binding units which still achieve successful infection.

FLEXIBLE AND RIGID BACKBONES

Optimal ligand densities on different scaffold architectures to achieve the high affinity with a particular spacer architecture is dependent on the preorganization or spatial orientation of ligands. Since flexible backbone and/or flexible linkers allow multivalent inhibitors to achieve different conformational shapes, the system has to lose much more conformational entropy to attach to the target surface for multivalent interactions. For instance, a divalent ligand connected by a

DOI: 10.1021/jacs.5b12950
J. Am. Chem. Soc. 2016, 138, 8654−8666

flexible spacer (such as OEG) will confer a favorable or unfavorable contribution to the binding energy depending on whether the spatial configuration matches the distance between the binding pockets between receptor units. A tight binding will then occur at the expense of entropy loss of the spacer. Consequently, the effectiveness of a divalent ligand is strongly connected to the nature of the spacer properties (flexibility, length, bond angles, etc.). Krishnamurthy et al. investigated the dependence of effective molarity for the intramolecular binding of a ligand covalently tethered to the surface with OEG spacers of different lengths ($(EG)_n$, with n = 0, 2, 5, 10, and 20).[126] They showed that the maximum effective molarity was attained when the spacer length matched the optimal length to allow the ligand to bind with the protein binding pocket. Calorimetry revealed that the enthalpic contacts of the flexible tethered OEG linker with the protein were not important, but the entropic cost for the binding was dominant. Furthermore, an unexpected weak dependence of the effective molarity on the spacer length was found for a spacer length surpassing the optimal size. Subsequently a theoretical study by Kane supported the latter observed weak dependency of free energy on multivalent binding on spacer length.[34] A very recent theoretical study on the influence of spacer length and flexibility on binding affinity during a multivalent interaction of a bivalent ligand and the influenza virus was given by Liese et al.[127] This study demonstrated a direct connection between the spacer length and flexibility and the binding affinity of the multivalent ligand. A central result of this theoretical study was that multivalency enhanced affinity, only if the dissociation constant of the monovalent ligand (K_{mono}) was lower than a critical value which referred to the critical dissociation constant K_{mono}*. K_{mono}* is the monovalent dissociation constant for a particular spacer length when monovalent and bivalent ligands bind equally well. If $K_{mono} < K_{mono}$*, a broader range of spacer lengths will exist for which divalent ligand binds better than the monovalent ligand. But if $K_{mono} > K_{mono}$*, the monovalent binds better because a loss in entropy of the spacer overcomes the gain in binding energy due to the multibinding of ligand units. This theoretical study was further expanded to understand the impact of stiff and flexible spacer for the divalent sialic acid ligand design for the binding with HA receptor protein on the influenza. The dissociation constant for binding of monomeric SA with HA is known to be 2.5 mM.[94] As per theoretical analysis, divalent SA ligand with the flexible PEG spacer is expected to bind less efficient than the monovalent SA. The stiff DNA spacer will enhance the binding affinity of the divalent SA than the monovalent SA, only if the length is optimized. Perfectly designed rigid linker for the divalent system will have higher affinity than the one with optimal flexible spacer. Another aspect to keep in mind is that flexible linkers can adopt a number of conformations without steric strain and can overcome steric obstruction in binding to the receptor sites whereas rigid linkers that are not perfectly designed cannot overcome steric obstruction.

In general, a multivalent ligand with a flexible spacer will initially promote the overall binding strength between two surfaces upon binding of the first ligand by reducing the spatial degrees of freedom of the ligands surrounding the one in the bound state. This will increase the binding probability of a second ligand to other receptor at the interface since the ligand concentration at the interface increases as well. The former situation invokes the rebinding effect in a divalent ligand while connected through a flexible spacer. Weber, Bujotzek, and Haag have provided a quantitative description of the rebinding effect for a monovalent and a bivalent ligand using a Markovian model.[128] Their results showed that the rebinding effect is present in both monovalent and bi-/multivalent ligand−receptor systems. The rebinding effect contribution toward binding depends on the energy barrier (activation barrier) between the bound and unbound states of the monovalent ligand. The energy barrier between bound and unbound state will be higher for a strongly bound monovalent ligand. Therefore, the rebinding effect will be negligible for a mono and multivalent system. In contrast, the energy barrier for a weak binding ligand between the bound and unbound states is reduced and the rebinding effect will be reinforced in both mono- and multivalent cases. For the very weakly bound ligand without any energy barrier, the effect of rebinding does not play a major role for the monovalent system but is strongly promoted in bi- and multivalent systems. The rebinding effect, therefore, has a significant contribution, if a high energy barrier between the unbound and bound state is missing. It is noteworthy that the "almost bound" state does not always represent an individual kinetic entity, so the applicability of the kinetic models including this state may be restricted to certain classes of ligand−receptor systems.

Although the entropy loss is not an issue when ligands are presented rigidly, optimum ligand density is a must to avoid a large loss of binding enthalpy. Optimum for the best binders is always a trade-off between the entropy loss and binding enthalpy; therefore, just enough flexibility for the attachment is needed. Linear polymers were extensively used in the past by Roy,[92,93] Whitesides,[129,49] and other groups.[130,131] Flexibility of the linear random coiled ligand architecture allows the system to attain different conformations for the maximum number of ligand−receptor interactions and steric shielding of some of the receptors. Since the affinity of ligands is greatly determined by the flexibility or rigidity of the polymeric backbone, this will further govern optimum ligand densities for a particular target. Dendritic polymer architectures have preoriented backbones in opposite to linear polymers. Hyperbranched polymers in the size range about 2−20 nm[132,133] with different statistical distribution of ligands can be synthesized with much less effort than perfect dendritic structures where the maximum size achieved is typically <10 nm. For example, conventional [G8] PAMAM has radii not more than 4 nm.[134−138] Biocompatible hyperbranched polymers can further be crossslinked to prepare 3D nano- and microgels. In a study by Steinhillber et al. polyglycerol particles were prepared on different length scales by extending the size of small hyperbranched polyglycerols (3 nm) to nanogels (32 nm) and microgels (140 and 220 μm) by miniemulsion and microfluidic templating, respectively.[139] These 3D gels are suitable for application as multivalent scaffold to bridge different length scales.

SIZE, STERIC SHIELDING, AND CLUSTERING EFFECT

Steric shielding has received much attention in recent decades to describe virus-antibody complexes.[140−142] It was then proposed that the finite size of an already bound antibody inherently overlaps other binding sites at the surface of the virus and therefore blocks additional antibody attachment. Scatchard plots, a plot of the ratio of bound antibody to the total antigen concentration (f) with the free antibody concentration (d), were initially used to extract the association constant (K) and the antigen valency (s). However,

DOI: 10.1021/jacs.5b12950
J. Am. Chem. Soc. 2016, 138, 8654−8666

experimental determination of valencies from antigen systems where the total number of binding units was previously known revealed that this value was about 1/3 lower than expected in the case of full antibody coating. Cowan and Underwood developed a detailed theoretical analysis to account for steric hindrance resulting from the interaction of monovalent ligands with a surface that presented multivalent antigenic units.[140] The central result from their model was that curved Scatchard plots were representative of systems where steric hindrance was present. However, their results were restricted to homogeneous monovalent ligands where the body of the binding unit was itself the cause of steric repulsion at the interface. This can drastically change if the scaffold and/or spacer is modified.

Taking the example of today's multivalent inhibitors, spherical multivalent inhibitors possessing hard or soft cores and displaying binding units at their surface have been synthesized and explored for their multivalent capacity. For example, Papp et al. showed the effective binding between sialic acid functionalized gold nanoparticles and the influenza virus.[143] These results showed, for the first time, the concomitant attachment of ligands to different receptors at the virus surface and pointed out the relevance of the contact area between an inhibitor and its target. The dependence on size for these types of rigid spherical inhibitors has been also investigated in our group by Vonnemann et al.[144] Polysulfated nanoparticle inhibitors smaller than the size of vesicular stomatitic virus (VSV), with a diameter ≥50 nm, inhibit the VSV-cell binding and thus the infection only to a small extent by multiple decoration of the virion. Meanwhile large-sized nanoparticle inhibitors (≥52 nm), which are of the same size of as the VSV virus, form VSV/NP clusters and effectively inhibit cell binding and infection. It is important to notice here that the particles greater than the size of virus do not benefit from this polyvalent enhancement effect, because there is no increase in the contact area between virus and the nanoparticle, which makes virus-sized nanoparticles the most efficient inhibitors.

The 1D platforms, such as peptide-based scaffolds, nanofibers, and carbon nanotubes, also can be used for anti-adhesive properties against pathogens as they provide multivalent interfaces for effective inhibition. Lee et al. observed enhanced *E. coli* bacterial cell agglutination with increasing lengths of the mannosylated nanofibers.[145] The length of the carbohydrate-coated nanofibers was controlled by coassembly of the amphiphile **1**, which had a highly crystalline aromatic core with the amphiphile **2**, which had a less crystalline aromatic core (see Figure 7).

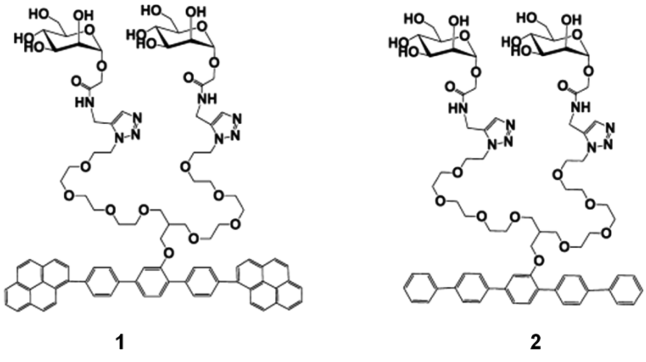

Figure 7. Chemical structures of amphiphiles **1** and **2**. Reprinted with permission from ref 145. Copyright 2012 American Chemical Society.

The length of the fibers decreased with the decreasing the crystallinity of aromatic core, i.e., by increasing the amount of amphiphile **2**. The 1-μm-sized fibers were able to form large-sized clusters of *E. coli* bacteria, while no bacterial agglutination was observed in fibers with a length lower than 70 nm. This indicated that the length of fiber plays a critical role in bacterial clustering and thus regulates its proliferation and agglutination (see Figure 8). Several other reports have also shown that glycosylated nanofibers can induce agglutination and thus inhibit the motility of pathogenic cells.[146,147]

To understand the combined effects of multivalency and steric shielding on pathogen inhibition, Vonnemann et al. proposed functionalized nanoparticles called "binders" instead of real viruses to offer a less complicated geometrical platform.[86] This study was based on the size of both strong and weak ligand/receptor pairs. Different sized streptavidin-coated silica nanoparticles (SA-NPs) were used as strong binding inhibitors for 10-μm-sized biotinylated silica particles. Dendritic polyglycerolsulfates (dPGs) and dPGS-coated gold nanoparticles (AuNP-dPGS) for L-selectin (L-sel)-coated binders were taken as an example for weak ligand/receptor pairs. The impact of the varying size and ligand density on the evaluation of IC_{50} was systematically investigated during inhibition. A modified version of the Cheng–Prusoff equation was proposed to account for the multivalent inhibitors covering the surface of the binder. In this equation $IC_{50} = K_d^{multi} + 0.5P[B]$, the first term is the contribution to multivalency and the prefactor of the binder concentration [B] accounts for the steric shielding contribution (see Figure 9). Their analysis concluded that the optimal size of the globular inhibitor should be smaller than that of the binder in most cases. The multivalent dissociation constant K_d^{multi} for large globular inhibitors exponentially depends on the contact area and is therefore much lower than the virus (pathogen) experimental/biological concentration, which shows the predominance of the steric shielding effect over multivalency in body fluids. The impact of steric shielding, furthermore, is only noticeable when all the inhibitors are bound to the pathogen.

Surface-functionalized dendritic polyglycerol architectures have also been used in the Haag group in the past few years. These soft scaffolds offer a competitive alternative to rigid-core spherical inhibitors. The elastic deformation increases their contact area, and thus multivalent binding is further enhanced. The physicochemical properties of these scaffolds could determine the unspecific adsorption at the interface. A dendritic inhibitor with a hydrophobic core then strongly adsorbs to the surface to decrease its solvation entropy ΔS_{solv}. The resulting binding affinity is then a balance between ligand density and the scaffold material/physicochemical properties. The potential of these dendritic inhibitors have been demonstrated in the case of dPGS by Dernedde et al. to inhibit inflammation.[148] The resulting binding interaction is then strongly influenced by the 3D shape and size of the scaffold, and the properties of the spacer will have severe consequences on the resulting binding strength between both interfaces.

MULTIVALENT PLATFORMS: FLEXIBILITY AND ADAPTABILITY

Besides globular inhibitors, large sheet-like scaffolds should potentially inhibit pathogen adhesion to a great extent, as they can provide much more contact area at interfaces. Adaptive multivalency, therefore, can be translated into larger sheets-like, 2-D multivalent scaffolds, with a high potential for targeting big

DOI: 10.1021/jacs.5b12950
J. Am. Chem. Soc. 2016, 138, 8654–8666

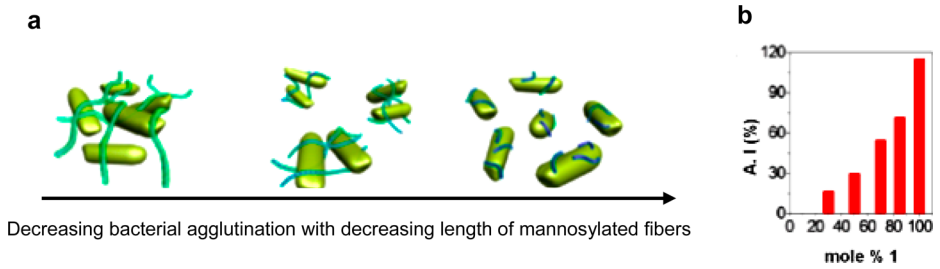

Figure 8. (a) Schematic for the regulation of agglutination and proliferation of bacterial cells by varying the nanofiber length. (b) Effect of the length of mannose-coated nanofibers on bacterial agglutination and proliferation. The degree of agglutination is represented by the agglutination index (AI). Adapted with permission from ref 145. Copyright 2012 American Chemical Society.

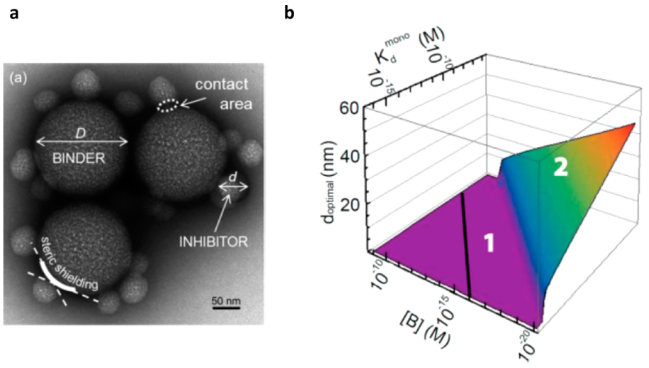

Figure 9. (a) TEM micrograph of d = 54 nm BT-NPs (inhibitors) incubated with D = 192 nm SA-NPs (binders) at a BT-NP/SA-NP concentration ratio of 15. Contact area, steric shielding area, and particle diameters are marked. (b) Predicted d/D ratios for globular inhibitors which result in the lowest required volume concentration of inhibitors to reduce the binding of a hypothetical binder (D = 100 nm) to its target surface by 50% dependent on K_d^{mono} and the binder concentration [B]. The graph can be divided into regimes in which (1) is a complete binding to the binder is even observed for the smallest possible inhibitor size and (2) in which larger inhibitor diameters are required for a complete binding of all inhibitors. The black solid line marks K_d^{mono} = [B]. Adapted with permission from ref 86. Copyright 2015 American Chemical Society.

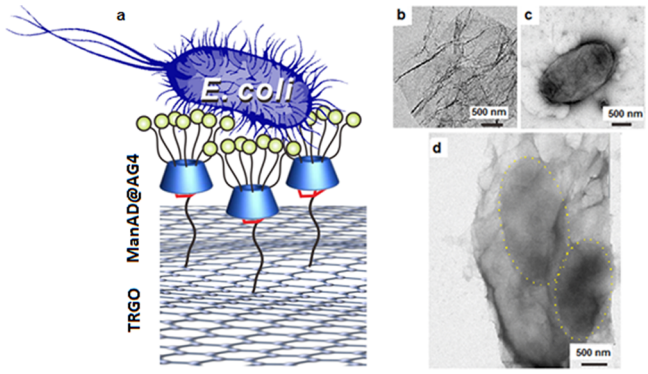

Figure 10. (a) Schematic representation for capturing *E. coli* by mannosylated cyclodextrin, adamantyl-functionalized (ManCD@AG4) graphene sheets. TEMs of the (b) ManCD-AG4 hybrid, (c) ORN178 *E. coli*, and (d) *E. coli* agglutination incubated with ManCD@AG4. The dashed yellow circles outline the captured bacteria. Adapted with permission from ref 27. Copyright 2015 American Chemical Society.

pathogens like bacteria or large viruses. Man-made Velcro is a common example of sheet-like multivalent platforms. Very recently our group showed the effectiveness of 2D functionalized thermally reduced graphene oxide (TRGO) sheets to trap and kill *E. coli* bacteria.[27] This multivalent mannosylated 2D platform was constructed by placing cyclodextrin-based sugar ligands (ManCD) on adamantyl-functionalized TRGO sheets (AG4). The unique IR absorption property of graphene materials was used to kill the captured bacteria by IR irradiation on the graphene−*E. coli* complex. This study promoted the remarkable capacity of functionalized graphene, due to its large surface area and flexibility to wrap large-sized pathogens (see Figure 10). Such micro- to nanometer range multivalent 2D lattices could be potentially used to sequester large viruses with a complex structure like the Ebola virus. Moreover, such molecular Velcro could find interesting future applications.

Graphene sheets, in general, are one-atom-thick 2D layers of sp^2-hybridized carbon atoms that are known for their thermal conductivity and mechanical stiffness.[149] Thin film particles of graphene oxide (GO) are highly flexible and can be synthesized in high yield.[150] In thermal/chemical reduction of GO,[151,152] some of the carbon atoms are sp^3 hybridized which makes it a flexible film bearing functionalizable hydroxyl groups. The reduced GO sheets can bend, extensively fold, and crumple. If the size of the sheet is much smaller than that of the pathogen, the sheet will bind and fully adhere on its surface. But if the surface area of the sheet is about the size of the pathogen or larger, then longitudinal binding will still occur to some extent, but transversal binding will require a high cost in bending energy. In this case, the material properties of the scaffold again play a central role. A general feature of graphene layers is that they can easily bend but not stretch. For a determined length vs width ratio, a graphene layer possesses a defined flexibility in solution which is defined by its bending rigidity. This property will change when the thickness of the graphene layer is modified for example by functionalization.[153] The functionalized graphene layer in solution possesses an intrinsic bending rigidity. Entrapment of pathogens with large sheets thus take place with an added topological restriction arising from the unfolded transversal section of the sheet which opposes deformation. These unbound sections of the sheet will block any further interactions with other interfaces upon contact.

The free binding energy is then given by the enormous solvation entropy due to water release and reorganization at the interface, the enthalpic contribution by the maximum array of binding pairs along the surface, and the high entropic cost due to configurational arrangement of the sheet during attachment. The thermodynamic aspect of interfacial binding forces, therefore, should be fully understood to generate effective multivalent interfaces. This involves not only the knowledge of the intrinsic binding strength between functional groups but also of the material properties and physicochemical behavior of the scaffold and spacer.

DOI: 10.1021/jacs.5b12950
J. Am. Chem. Soc. 2016, 138, 8654−8666

We expect a wider repertoire of multivalent architectures, beyond the already explored to date, and will follow and improve their efficacy as inhibitors. For example, the functionalized carbon sheets, gold nanorods, and other stimuli-responsive nanocomposites (pH, ionic strength, temperature, etc.) with multivalent interfaces will impose new additional parameters on the binding free energy.[154]

CONCLUSION AND PERSPECTIVE

Developing a successful multivalent inhibitor requires a detailed understanding of the biological interface to be targeted. Carrier backbone, size, linker, ligand density, and also mechanical properties are important parameters that need to be optimized for the respective multivalent inhibitor. Besides high binding affinities, other mechanisms such as steric shielding and clustering effects are crucial for successful pathogen inhibition. There are pros and cons associated with each class of multivalent inhibitor and the complexity at multivalent interfaces increases going from small defined to larger sized scaffolds. Also lower ligand densities on larger scaffolds can be preferable and even stronger effects have been observed as compared to high ligand density. Even after successfully trapping or inhibiting the pathogen *in vitro*, several questions remain when translating the concept into an *in vivo* situation. The most important is the issue of toxicity and clearance. The fate of the inhibitor−pathogen complex also needs to be addressed, if they can be uptaken by macrophages and excreted as a complex from the body. Despite their high efficacy, so far only a few multivalent inhibitors have been tested *in vivo* because of the toxicity of many inhibitors and scaffolds. Also, not many reports are available on the applicability of such inhibitors in advanced stages of infection. Therefore, the applicability of multivalent inhibitors as drugs or prophylactics has a great potential for the future.

AUTHOR INFORMATION

Corresponding Author

*haag@chemie.fu-berlin.de

Notes

The authors declare no competing financial interest.

ACKNOWLEDGMENTS

We thank the Deutsche Forschungsgemeinschaft (DFG) for financial support within the Collaborative Research Centre 765, where different biophysical methods are being used to understand multivalency quantitatively at the molecular level and the knowledge gained is applied to design novel multivalent inhibitors. We are grateful to Dr. Pamela Winchester for careful language editing and Dr. Wiebke Fischer for support with designing the graphics. We also acknowledge Dr. Christoph Böttcher and Dr. Kai Ludwig for providing the cryo-TEM image of influenza A virus in Figure 2a.

REFERENCES

(1) Fasting, C.; Schalley, C. A.; Weber, M.; Seitz, O.; Hecht, S.; Koksch, B.; Dernedde, J.; Graf, C.; Knapp, E.-W.; Haag, R. *Angew. Chem., Int. Ed.* **2012**, *51*, 10419.
(2) Bhatia, S.; Dimde, M.; Haag, R. *MedChemComm* **2014**, *5*, 862.
(3) Ting, S. R. S.; Chen, G.; Stenzel, M. H. *Polym. Chem.* **2010**, *1*, 1392.
(4) Ullrich, A.; Schlessinger, J. *Cell* **1990**, *61*, 203.
(5) Schlessinger, J. *Cell* **2000**, *103*, 211.
(6) Dubois, P. M.; Stepinski, J.; Urbain, J.; Sibley, C. H. *Eur. J. Immunol.* **1992**, *22*, 851.
(7) Jiang, W.; Kim, B. Y.; Rutka, J. T.; Chan, W. C. *Nat. Nanotechnol.* **2008**, *3*, 145.
(8) Bhella, D. *Philos. Trans. R. Soc., B* **2015**, *370*, 20140035.
(9) Grove, J.; Marsh, M. *J. Cell Biol.* **2011**, *195*, 1071.
(10) Krachler, A. M.; Ham, H.; Orth, K. *Proc. Natl. Acad. Sci. U. S. A.* **2011**, *108*, 11614.
(11) Pizarro-Cerda, J.; Cossart, P. *Cell* **2006**, *124*, 715.
(12) Serrano-Gomez, D.; Dominguez-Soto, A.; Ancochea, J.; Jimenez-Heffernan, J. A.; Leal, J. A.; Corbi, A. L. *J. Immunol.* **2004**, *173*, 5635.
(13) Mendes-Giannini, M. J.; Soares, C. P.; da Silva, J. L. M.; Andreotti, P. F. *FEMS Immunol. Med. Microbiol.* **2005**, *45*, 383.
(14) Bernardi, A.; Jiménez-Barbero, J.; Casnati, A.; De Castro, C.; Darbre, T.; Fieschi, F.; Finne, J.; Funken, H.; Jaeger, K.-E.; Lahmann, M.; Lindhorst, T. K.; Marradi, M.; Messner, P.; Molinaro, A.; Murphy, P. V.; Nativi, C.; Oscarson, S.; Penadés, S.; Peri, F.; Pieters, R. J.; Renaudet, O.; Reymond, J.-L.; Richichi, B.; Rojo, J.; Sansone, F.; Schäffer, C.; Turnbull, W. B.; Velasco-Torrijos, T.; Vidal, S.; Vincent, S.; Wennekes, T.; Zuilhof, H.; Imberty, A. *Chem. Soc. Rev.* **2013**, *42*, 4709.
(15) Weis, W.; Brown, J. H.; Cusack, S.; Paulson, J. C.; Skehel, J. J.; Wiley, D. C. *Nature* **1988**, *333*, 426.
(16) van Kooyk, Y.; Geijtenbeek, T. B. H. *Nat. Rev. Immunol.* **2003**, *3*, 697.
(17) Gilboa-Garber, N. *Methods Enzymol.* **1982**, *83*, 378.
(18) Imberty, A.; Wimmerová, M.; Mitchell, E. P.; Gilboa-Garber, N. *Microbes Infect.* **2004**, *6*, 221.
(19) Heidecke, C. D.; Lindhorst, T. K. *Chem. - Eur. J.* **2007**, *13*, 9056.
(20) Lane, M. C.; Mobley, H. L. T. *Kidney Int.* **2007**, *72*, 19.
(21) Fan, E.; Merritt, E. A.; Verlinde, C. L. M. J.; Hol, W. G. J. *Curr. Opin. Struct. Biol.* **2000**, *10*, 680.
(22) Ling, H; Boodhoo, A.; Hazes, B.; Cummings, M. D.; Armstrong, G. D.; Brunton, J. L.; Read, R. J. *Biochemistry* **1998**, *37*, 1777.
(23) Moscona, A. *Annu. Rev. Med.* **2008**, *59*, 397.
(24) Schirmer, P.; Holodniy, M. *Expert Opin. Drug Saf.* **2009**, *8*, 357.
(25) Papp, I.; Sieben, C.; Sisson, A. L.; Kostka, J.; Böttcher, C.; Ludwig, K.; Herrmann, A.; Haag, R. *ChemBioChem* **2011**, *12*, 887.
(26) Reuter, J. D.; Myc, A.; Hayes, M. M.; Gan, Z.; Roy, R.; Qin, D.; Yin, R.; Piehler, L. T.; Esfand, R.; Tomalia, D. A.; Baker, J. R., Jr. *Bioconjugate Chem.* **1999**, *10*, 271.
(27) Qi, Z.; Bharate, P.; Lai, C. H.; Ziem, B.; Böttcher, C.; Schulz, A.; Beckert, F.; Hatting, B.; Mulhaupt, R.; Seeberger, P. H.; Haag, R. *Nano Lett.* **2015**, *15*, 6051.
(28) Lee, C. M.; Weight, A. K.; Haldar, J.; Wang, L.; Klibanov, A. M.; Chen, J. *Proc. Natl. Acad. Sci. U. S. A.* **2012**, *109*, 20385.
(29) Dernedde, J.; Rausch, A.; Weinhart, M.; Enders, S.; Tauber, R.; Licha, K.; Schirner, M.; Zugel, U.; von Bonin, A.; Haag, R. *Proc. Natl. Acad. Sci. U. S. A.* **2010**, *107*, 19679.
(30) Durka, M.; Buffet, K.; Iehl, J.; Holler, M.; Nierengarten, J.-F.; Taganna, J.; Bouckaert, J.; Vincent, S. P. *Chem. Commun.* **2011**, *47*, 1321.
(31) Xia, Z.; Triffitt, J. T. *Biomed. Mater.* **2006**, *1*, R1.
(32) Anderson, J. M.; Rodriguez, A.; Chang, D. T. *Semin. Immunol.* **2008**, *20*, 86.
(33) Longmire, M.; Choyke, P. L.; Kobayashi, H. *Nanomedicine (London, U. K.)* **2008**, *3*, 703.
(34) Kane, R. S. *Langmuir* **2010**, *26*, 8636.
(35) Kitov, P. I.; Bundle, D. R. *J. Am. Chem. Soc.* **2003**, *125*, 16271.
(36) Gambaryan, A. S.; Tuzikov, A. B.; Chinarev, A. A.; Juneja, L. R.; Bovin, N. V.; Matrosovich, M. N. *Antiviral Res.* **2002**, *55*, 201.
(37) Landers, J. J.; Cao, Z.; Lee, I.; Piehler, L. T.; Myc, P. P.; Myc, A.; Hamouda, T.; Galecki, A. T.; Baker, J. R., Jr. *J. Infect. Dis.* **2002**, *186*, 1222.
(38) Karlsson, K.-A. *Mol. Microbiol.* **1998**, *29*, 1.
(39) Armstrong, G. D.; Fodor, E.; Vanmaele, R. *J. Infect. Dis.* **1991**, *164*, 1160.

DOI: 10.1021/jacs.5b12950
J. Am. Chem. Soc. 2016, 138, 8654−8666

(40) Armstrong, G. D.; McLaine, P. N.; Rowe, P. C. Clinical trials of Synsorb-Pk in preventing hemolytic-uremic syndrome. In *Escherichia coli O157:H7 and Other Shiga Toxin-producing E. coli Strains*; Kaper, J. B., O'Brien, A. D., Eds.; American Society for Microbiology: Washington, DC, 1998; p 374.
(41) Rowe, P. C.; Milner, R.; Orrbine, E.; Klassen, T. P.; Goodyer, P. G.; MacKenzie, A. M.; Wells, G. A.; Auclair, F.; Blanchard, C.; Lior, H.; Rafter, D. J.; McLaine, P. N.; Armstrong, G. D. *Pediatr. Res.* **1997**, *41*, 283.
(42) Takeda, T.; Yoshino, K.; Adachi, E.; Sato, Y.; Yamagata, K. *Microbiol. Immunol.* **1999**, *43*, 331.
(43) Pinyon, R. A.; Paton, J. C.; Paton, A. W.; Botten, J. A.; Morona, R. *J. Infect. Dis.* **2004**, *189*, 1547.
(44) Paton, A. W.; Morona, R.; Paton, J. C. *Nat. Med.* **2000**, *6*, 265.
(45) Zuercher, A. W.; Horn, M. P.; Que, J. U.; Ruedeberg, A.; Schoeni, M. H.; Schaad, U. B.; Marcus, P.; Lang, A. B. *FEMS Immunol. Med. Microbiol.* **2006**, *47*, 302.
(46) Chang, C. E.; Chen, W.; Gilson, M. K. *Proc. Natl. Acad. Sci. U. S. A.* **2007**, *104*, 1534.
(47) Bronowska, A. K. Thermodynamics of Ligand-Protein Interactions: Implications for Molecular Design. In *Thermodynamics - Interaction Studies - Solids, Liquids and Gases*;Moreno Piraján, J. C., Ed.; InTech, 2011; DOI: 10.5772/19447.
(48) Olsson, T. S.; Williams, M. A.; Pitt, W. R.; Ladbury, J. E. *J. Mol. Biol.* **2008**, *384*, 1002.
(49) Mammen, M.; Choi, S.-K.; Whitesides, G. M. *Angew. Chem., Int. Ed.* **1998**, *37*, 2754.
(50) Badjić, J. D.; Nelson, A.; Cantrill, S. J.; Turnbull, W. B.; Stoddart, J. F. *Acc. Chem. Res.* **2005**, *38*, 723.
(51) Mulder, A.; Huskens, J.; Reinhoudt, D. N. *Org. Biomol. Chem.* **2004**, *2*, 3409.
(52) Huskens, J.; Mulder, A.; Auletta, T.; Nijhuis, C. A.; Ludden, M. J. W.; Reinhoudt, D. N. *J. Am. Chem. Soc.* **2004**, *126*, 6784.
(53) Schneider, H. J. *Angew. Chem., Int. Ed.* **2009**, *48*, 3924.
(54) Dam, T. K.; Roy, R.; Page, D.; Brewer, C. F. *Biochemistry* **2002**, *41*, 1351.
(55) del Mar Hernández, M.; José, M. V. *Anal. Biochem.* **2003**, *313*, 226.
(56) Doyle, M. L. *Curr. Opin. Biotechnol.* **1997**, *8*, 31.
(57) Ladbury, J. E.; Chowdhry, B. Z. *Chem. Biol.* **1996**, *3*, 791.
(58) Leavitt, S.; Freire, E. *Curr. Opin. Struct. Biol.* **2001**, *11*, 560.
(59) Pierce, M. M.; Raman, C. S.; Nall, B. T. *Methods* **1999**, *19*, 213.
(60) Critchley, P.; Willand, M. N.; Rullay, A. K.; Crout, D. H. G. *Org. Biomol. Chem.* **2003**, *1*, 928.
(61) Stahelin, R. V. *Mol. Biol. Cell* **2013**, *24*, 883.
(62) Patching, S. G. *Biochim. Biophys. Acta, Biomembr.* **2014**, *1838*, 43.
(63) Dixon, M. C. *J. Biomol. Technol.* **2008**, *19*, 151.
(64) Janshoff, A.; Galla, H.-J.; Steinem, C. *Angew. Chem., Int. Ed.* **2000**, *39*, 4004.
(65) Marx, K. A. *Biomacromolecules* **2003**, *4*, 1099.
(66) Seidel, S. A. I.; Dijkman, P. M.; Lea, W. A.; van den Bogaart, G.; Jerabek-Willemsen, M.; Lazic, A.; Joseph, J. S.; Srinivasan, P.; Baaske, P.; Simeonov, A.; Katritch, I.; Melo, F. A.; Ladbury, J. E.; Schreiber, G.; Watts, A.; Braun, D.; Duhr, S. *Methods* **2013**, *59*, 301.
(67) Seidel, S. A. I.; Wienken, C. J.; Geissler, S.; Jerabek-Willemsen, M.; Duhr, S.; Reiter, A.; Trauner, D.; Braun, D.; Baaske, P. *Angew. Chem., Int. Ed.* **2012**, *51*, 10656.
(68) Zillner, K.; Jerabek-Willemsen, M.; Duhr, S.; Braun, D.; Längst, G.; Baaske, P. In *Functional Genomics*; Kaufmann, M., Klinger, C., Eds.; Springer: New York, 2012; Vol. *815*, p 241.
(69) Israelachvili, J. N.; Leckband, D.; Schmitt, F.-J.; Zasadzinski, J.; Walker, S.; Chiruvolu, S. *Methods For Studying Cell Adhesion*; Springer Verlag: Berlin, 1993; p 37.
(70) Wong, J. Y.; Kuhl, T. L.; Israelachvili, J. N.; Mullah, N.; Zalipsky, S. *Science* **1997**, *275*, 820.
(71) Brampton, C.; Wahab, O.; Batchelor, M.; Allen, S.; Williams, P. *Eur. Biophys. J.* **2011**, *40*, 247.
(72) Gourier, C.; Jegou, A.; Husson, J.; Pincet, F. *Cell. Mol. Bioeng.* **2008**, *1*, 263.
(73) Hugel, T.; Seitz, M. *Macromol. Rapid Commun.* **2001**, *22*, 989.
(74) Willemsen, O. H.; Snel, M. M. E.; Cambi, A.; Greve, J.; De Grooth, B. G.; Figdor, C. G. *Biophys. J.* **2000**, *79*, 3267.
(75) Capitanio, M.; Pavone, F. S. *Biophys. J.* **2013**, *105*, 1293.
(76) Neuman, K. C.; Nagy, A. *Nat. Methods* **2008**, *5*, 491.
(77) Bell, G. I. *Science* **1978**, *200*, 618.
(78) Evans, E.; Ritchie, K. *Biophys. J.* **1997**, *72*, 1541.
(79) Rankl, C.; Kienberger, F.; Wildling, L.; Wruss, J.; Gruber, H. J.; Blaas, D.; Hinterdorfer, P. *Proc. Natl. Acad. Sci. U. S. A.* **2008**, *105*, 17778.
(80) Le, D. T.; Guérardel, Y.; Loubière, P.; Mercier-Bonin, M.; Dague, E. *Biophys. J.* **2011**, *101*, 2843.
(81) Kim, Y.; Cao, Z.; Tan, W. *Proc. Natl. Acad. Sci. U. S. A.* **2008**, *105*, 5664.
(82) Li, M.-H.; Choi, S. K.; Leroueil, P. R.; Baker, J. R., Jr. *ACS Nano* **2014**, *8*, 5600.
(83) Tassa, C.; Duffner, J. L.; Lewis, T. A.; Weissleder, R.; Schreiber, S. L.; Koehler, A. N.; Shaw, S. Y. *Bioconjugate Chem.* **2010**, *21*, 14.
(84) Munoz, E. M.; Correa, J.; Riguera, R.; Fernandez-Megia, E. *J. Am. Chem. Soc.* **2013**, *135*, 5966.
(85) Gestwicki, J. E.; Cairo, C. W.; Strong, L. E.; Oetjen, K. A.; Kiessling, L. L. *J. Am. Chem. Soc.* **2002**, *124*, 14922.
(86) Vonnemann, J.; Liese, S.; Kuehne, C.; Ludwig, K.; Dernedde, J.; Böttcher, C.; Netz, R.; Haag, R. *J. Am. Chem. Soc.* **2015**, *137*, 2572.
(87) Yamaguchi, M.; Danev, R.; Nishiyama, K.; Sugawara, K.; Nagayama, K. *J. Struct. Biol.* **2008**, *162*, 271.
(88) Ruigrok, R. W. H.; Calder, L. J.; Wharton, S. A. *Virology* **1989**, *173*, 311.
(89) Ruigrok, R. W. H.; Andree, P. J.; Hooft Van Huysduynen, R. A. M.; Mellema, J. E. *J. Gen. Virol.* **1984**, *65*, 799.
(90) Li, S.; Sieben, C.; Ludwig, K.; Höfer, C. T.; Chiantia, S.; Herrmann, A.; Eghiaian, F.; Schaap, I. A. *Biophys. J.* **2014**, *106*, 1447.
(91) Böttcher, C.; Ludwig, K.; Herrmann, A.; van Heel, M.; Stark, H. *FEBS Lett.* **1999**, *463*, 255.
(92) Roy, R.; Pon, R. A.; Tropper, F. D.; Andersson, F. O. *J. Chem. Soc., Chem. Commun.* **1993**, 264.
(93) Roy, R.; Andersson, F. O.; Harms, G.; Kelm, S.; Schauer, R. *Angew. Chem., Int. Ed. Engl.* **1992**, *31*, 1478.
(94) Lees, W. J.; Spaltenstein, A.; Kingery-Wood, J. E.; Whitesides, G. M. *J. Med. Chem.* **1994**, *37*, 3419.
(95) Glick, G. D.; Knowles, J. R. *J. Am. Chem. Soc.* **1991**, *113*, 4701.
(96) Rao, J.; Lahiri, J.; Weis, R. M.; Whitesides, G. M. *J. Am. Chem. Soc.* **2000**, *122*, 2698.
(97) Waldmann, M.; Jirmann, R.; Hoelscher, K.; Wienke, M.; Niemeyer, F. C.; Rehders, D.; Meyer, B. *J. Am. Chem. Soc.* **2014**, *136*, 783.
(98) Ohta, T.; Miura, N.; Fujitani, N.; Nakajima, F.; Niikura, K.; Sadamoto, R.; Guo, C. T.; Suzuki, T.; Suzuki, Y.; Monde, K.; Nishimura, S. *Angew. Chem., Int. Ed.* **2003**, *42*, 5186.
(99) Oesterhelt, F.; Rief, M.; Gaub, H. E. *New J. Phys.* **1999**, *1*, 6.
(100) Kreuzer, H. J.; Wang, R. L. C.; Grunze, M. *New J. Phys.* **1999**, *1*, 21.
(101) Bujotzek, A.; Shan, M.; Haag, R.; Weber, M. *J. Comput.-Aided Mol. Des.* **2011**, *25*, 253.
(102) Shan, M.; Carlson, K. E.; Bujotzek, A.; Wellner, A.; Gust, R.; Weber, M.; Katzenellenbogen, J. A.; Haag, R. *ACS Chem. Biol.* **2013**, *8*, 707.
(103) Abendroth, F.; Bujotzek, A.; Shan, M.; Haag, R.; Weber, M.; Seitz, O. *Angew. Chem., Int. Ed.* **2011**, *50*, 8592.
(104) Branson, T. R.; McAllister, T. E.; Garcia-Hartjes, J.; Fascione, M. A.; Ross, J. F.; Warriner, S. L.; Wennekes, T.; Zuilhof, H.; Turnbull, W. B. *Angew. Chem., Int. Ed.* **2014**, *53*, 8323.
(105) Kitov, P. I.; Sadowska, J. M.; Mulvey, G.; Armstrong, G. D.; Ling, H.; Pannu, N. S.; Read, R. J.; Bundle, D. R. *Nature* **2000**, *403*, 669.
(106) Levine, P. M.; Carberry, T. P.; Holub, J. M.; Kirshenbaum, K. *MedChemComm* **2013**, *4*, 493.

DOI: 10.1021/jacs.5b12950
J. Am. Chem. Soc. 2016, 138, 8654−8666

(107) Zhang, Z.; Merritt, E. A.; Ahn, M.; Roach, C.; Hou, Z.; Verlinde, C. L. M. J.; Hol, W. G. J.; Fan, E. *J. Am. Chem. Soc.* **2002**, *124*, 12991.
(108) Merritt, E. A.; Zhang, Z.; Pickens, J. C.; Ahn, M.; Hol, W. G. J.; Fan, E. *J. Am. Chem. Soc.* **2002**, *124*, 8818.
(109) Branson, T. R.; Turnbull, W. B. *Chem. Soc. Rev.* **2013**, *42*, 4613.
(110) Jacobson, J. M.; Yin, J.; Kitov, P. I.; Mulvey, G.; Griener, T. P.; James, M. N. G.; Armstrong, G.; Bundle, D. R. *J. Biol. Chem.* **2014**, *289*, 885.
(111) Tsutsuki, K.; Watanabe-Takahashi, M.; Takenaka, Y.; Kita, E.; Nishikawa, K. *Infect. Immun.* **2013**, *81*, 2133.
(112) Kitov, P. I.; Bundle, D. R. *J. Am. Chem. Soc.* **2003**, *125*, 16271.
(113) Sisu, C.; Baron, A. J.; Branderhorst, H. M.; Connell, S. D.; Weijers, C. A. G. M.; de Vries, R.; Hayes, E. D.; Pukin, A. V.; Gilbert, M.; Pieters, R. J.; Zuilhof, H.; Visser, G. M.; Turnbull, W. B. *ChemBioChem* **2009**, *10*, 329.
(114) Fu, O.; Pukin, A. V.; van Ufford, H. C.; Branson, T. R.; Thies-Weesie, D. M.; Turnbull, W. B.; Visser, G. M.; Pieters, R. J. *ChemistryOpen* **2015**, *4*, 471.
(115) Jayaraman, A.; Hall, C. K.; Genzer, J. *Biophys. J.* **2006**, *91*, 2227.
(116) Moore, N. W.; Kuhl, T. L. *Biophys. J.* **2006**, *91*, 1675.
(117) Jeppesen, C.; Wong, J. Y.; Kuhl, T. L.; Israelachvili, J. N.; Mullah, N.; Zalipsky, S.; Marques, C. M. *Science* **2001**, *293*, 465.
(118) Kol, N.; Gladnikoff, M.; Barlam, D.; Shneck, R. Z.; Rein, A.; Rousso, I. *Biophys. J.* **2006**, *91*, 767.
(119) Kol, N.; Shi, Y.; Tsvitov, M.; Barlam, D.; Shneck, R. Z.; Kay, M. S.; Rousso, I. *Biophys. J.* **2007**, *92*, 1777.
(120) Li, S.; Eghiaian, F.; Sieben, C.; Herrmann, A.; Schaap, I. A. T. *Biophys. J.* **2011**, *100*, 637.
(121) Schaap, I. A. T.; Eghiaian, F.; des Georges, A.; Veigel, C. *J. Biol. Chem.* **2012**, *287*, 41078.
(122) Cuellar, J. L.; Meinhoevel, F.; Hoehne, M.; Donath, E. *J. Gen. Virol.* **2010**, *91*, 2449.
(123) Rankl, C.; Kienberger, F.; Wildling, L.; Wruss, J.; Gruber, H. J.; Blaas, D.; Hinterdorfer, P. *Proc. Natl. Acad. Sci. U. S. A.* **2008**, *105*, 17778.
(124) Herrmann, A.; Sieben, C. *Integr. Biol.* **2015**, *7*, 620.
(125) Sieben, C.; Kappel, C.; Zhu, R.; Wozniak, A.; Rankl, C.; Hinterdorfer, P.; Grubmüller, H.; Herrmann, A. *Proc. Natl. Acad. Sci. U. S. A.* **2012**, *109*, 13626.
(126) Krishnamurthy, V. M.; Semetey, V.; Bracher, P. J.; Shen, N.; Whitesides, G. M. *J. Am. Chem. Soc.* **2007**, *129*, 1312.
(127) Liese, S.; Netz, R. *Beilstein J. Org. Chem.* **2015**, *11*, 804.
(128) Weber, M.; Bujotzek, A.; Haag, R. *J. Chem. Phys.* **2012**, *137*, 054111.
(129) Sigal, G. B.; Mammen, M.; Dahmann, G.; Whitesides, G. M. *J. Am. Chem. Soc.* **1996**, *118*, 3789.
(130) Kiessling, L. L.; Gestwicki, J. E.; Strong, E. L. *Curr. Opin. Chem. Biol.* **2000**, *4*, 696.
(131) Kanai, M.; Mortell, K. H.; Kiessling, L. L. *J. Am. Chem. Soc.* **1997**, *119*, 9931.
(132) Staedtler, A. M.; Hellmund, M.; Sheikhi Mehrabadi, F.; Thota, B. N. S.; Zollner, T. M.; Koch, M.; Haag, R.; Schmidt, N. *J. Mater. Chem. B* **2015**, *3*, 8993.
(133) Kainthan, R. K.; Muliawan, E. B.; Hatzikiriakos, S. G.; Brooks, D. E. *Macromolecules* **2006**, *39*, 7708.
(134) Mansfield, M. L.; Klushin, L. I. *J. Phys. Chem.* **1992**, *96*, 3994.
(135) Murat, M.; Grest, G. S. *Macromolecules* **1996**, *29*, 1278.
(136) Stechemesser, S.; Eimer, W. *Macromolecules* **1997**, *30*, 2204.
(137) Tomalia, D. A. *High Perform. Polym.* **2001**, *13*, S1.
(138) Newkome, G. R.; Shreiner, C. D. *Polymer* **2008**, *49*, 1.
(139) Steinhilber, D.; Seiffert, S.; Heyman, J. A.; Paulus, F.; Weitz, D. A.; Haag, R. *Biomaterials* **2011**, *32*, 1311.
(140) Cowan, R.; Underwood, P. A. *J. Theor. Biol.* **1988**, *132*, 319.
(141) Pellequer, J. L.; Van Regenmortel, M. H. V. *Mol. Immunol.* **1993**, *30*, 955.
(142) Hlavacek, W. S.; Posner, R. G.; Perelson, A. S. *Biophys. J.* **1999**, *76*, 3031.
(143) Papp, I.; Sieben, C.; Ludwig, K.; Roskamp, M.; Böttcher, C.; Schlecht, S.; Herrmann, A.; Haag, R. *Small* **2010**, *6*, 2900.
(144) Vonnemann, J.; Sieben, C.; Wolff, C.; Ludwig, K.; Böttcher, C.; Herrmann, A.; Haag, R. *Nanoscale* **2014**, *6*, 2353.
(145) Lee, D. W.; Kim, T.; Park, I. S.; Huang, Z.; Lee, M. *J. Am. Chem. Soc.* **2012**, *134*, 14722.
(146) Ryu, J.-H.; Lee, E.; Lim, Y.-B.; Lee, M. *J. Am. Chem. Soc.* **2007**, *129*, 4808.
(147) Lim, Y. B.; Lee, E.; Lee, M. *Macromol. Rapid Commun.* **2011**, *32*, 191.
(148) Dernedde, J.; Rausch, A.; Weinhart, M.; Enders, S.; Tauber, R.; Licha, K.; Schirner, M.; Zügel, U.; von Bonin, A.; Haag, R. *Proc. Natl. Acad. Sci. U. S. A.* **2010**, *107*, 19679.
(149) Stankovich, S.; Dikin, D. A.; Dommett, G. H.; Kohlhaas, K. M.; Zimney, E. J.; Stach, E. A.; Piner, R. D.; Nguyen, S. T.; Ruoff, R. S. *Nature* **2006**, *442*, 282.
(150) Hirata, M.; Gotou, T.; Horiuchi, S.; Fujiwara, M.; Ohba, M. *Carbon* **2004**, *42*, 2929.
(151) Chua, C. K.; Pumera, M. *Chem. Soc. Rev.* **2014**, *43*, 291.
(152) Huh, S. H. Thermal Reduction of Graphene Oxide. In *Physics and Applications of Graphene - Experiments*; Mikhailov, S., Ed.; InTech, 2011; DOI: 10.5772/14156.
(153) Schniepp, H. C.; Kudin, K. N.; Li, J.-L.; Prud'homme, R. K.; Car, R.; Saville, D. A.; Aksay, I. A. *ACS Nano* **2008**, *2*, 2577.
(154) Schwarz, U. *Physik J.* **2015**, *14*, 29.

DOI: 10.1021/jacs.5b12950
J. Am. Chem. Soc. 2016, 138, 8654−8666